EUROPEAN COMMISSION
Community Research

SEVENTH FRAMEWORK PROGRAMME

CARBOWASTE

Treatment and Disposal of Irradiated Graphite and Other Carbonaceous Waste

Grant Agreement Number: FP7-211333

Deliverable D-3.3.2

Report on analysis of impurity and isotope sites before and after treatment

Author(s):

Katrin Baginski, Werner von Lensa, Dirk Vulpius;
Forschungszentrum Juelich GmbH

Abbie Jones; University of Manchester

Document Number: CARBOWASTE-D-0912-3.3.2
Date of issue of this report : 18/12/2009

Start date of project : **01/04/2008** Duration : **48 Months**

Distribution list

Person and organisation name and/or group	Comments
Task 3.3 members	
Executive Board	
Co-ordinator	

Project co-funded by the European Commission under the Seventh Framework Programme (2007 to 2011) of the European Atomic Energy Community (EURATOM) for nuclear research and training activities		
Dissemination Level		
PU	Public	
RE	Restricted to the partners of the CARBOWASTE project	
CO	Confidential, only for specific distribution list defined on this document	**X**

CARBOWASTE		
Work package: 3 **Task: :** 3.3	**CARBOWASTE document no:** CARBOWASTE-0912-D-3.3.2 (e.g. May 2008 as date of issue: 0805)	**Document type:** D=Deliverable
Issued by: Forschungszentrum Juelich GmbH (DE) **Internal no.:** CW1001-Deliverable-3-3-2-b		**Document status:** DRAFT

Document title

Report on analysis of impurity and isotope sites before and after treatment

Executive summary

There are many types and sources of irradiated nuclear graphite waste and therefore it is unlikely a comprehensive database of empirical data for all this waste could ever be achieved. Therefore to gain an understanding of the location and stability of impurities / radioactive isotopes in selected irradiated graphite waste before and after various treatments. The latest scientific techniques will be employed to investigate where and how impurities / radioactive isotopes are located within virgin and irradiated nuclear graphite. Thus leading to a robust understanding of the value of various treatment options.

This understanding may then be called upon in deciding and validating the most appropriate options for the disposal of irradiated nuclear graphite waste, so that it is also valid to evaluate the direct disposal of graphite without treatment. The results that come out from this task will also be added to the characteristics database in |Task 3.2 and 3.5.

In this Task UoM, CIEMAT, FZJ work in characterisation after and before treatment. CEA, SCK·CEN, INR participate in the characterisation of their waste forms without treatment. WP6 has been involved to provide evaluation criteria for direct disposal.

Revisions

Rev.	Date	Short description	Author	Review	Task Leader	WP Leader
00	dd/mm/yyyy	Issue	Name, Organisation	Name, Organisation *Signature*	Name, Organisation *Signature*	Name, Organisation *Signature*
01	dd/mm/yyyy	First issue	Vulpius FZJ	Jones UoM	Vulpius FZJ	Pina CIEMAT
02	18/12/2009	2nd Issue	Jones UoM	Vulpius FZJ	Jones UoM	Pina CIEMAT

Table of Contents

1. Objectives of the Task

There are many types and sources of irradiated nuclear graphite waste and therefore it is unlikely a comprehensive database of empirical data for all this waste could ever be achieved. Therefore to gain an understanding of the location and stability of impurities / radioactive isotopes in selected irradiated graphite waste before and after various treatments. The latest scientific techniques will be employed to investigate where and how impurities / radioactive isotopes are located within virgin and irradiated nuclear graphite. Thus, extensive information will be supplied, which will lead to a more robust understanding of the value of various treatment and disposal options.

This understanding may then be called upon in deciding and validating the most appropriate options for the disposal of irradiated nuclear graphite waste, so that it is also valid to evaluate the direct disposal of graphite without treatment. The results that come out from this task will also be added to the characteristics database in task 3.2 and 3.5.

The most important feature of irradiated graphite is the chemical purity of the original graphite. The initial chemical composition fundamentally controls the isotopes that become activated on irradiation, and hence determines the radionuclide inventory, and the ease with which it may be managed or disposed.

The radionuclide inventory of graphite is dominated by H-3, C-14 and Cl-36 [**Erreur ! Signet non défini.**].

2. Activation Processes & Chemical Reactions

2.1 Tritium

Tritium is created throughout the graphite from lithium impurities, and diffuses at a slow rate to reach pore surfaces where it exchanges with adsorbed hydrogen bearing molecules. Adventitious tritium from ternary fission events will also tend to become absorbed at the pore surfaces. Release in normal operation then occurs through exchange with hydrogen bearing molecules in the coolant (hydrogen, water and methane in CO2-cooled systems), creating a quasi ‘steady state’ [iii].

2.2 Radiocarbon

The dominant route for formation of C-14 is previously speculated to be dominated via the reaction N-14(n,p)C-14. Nitrogen is incorporated into the graphite matrix because graphite manufacture is typically done in air. Nitrogen may also be present in varying concentrations in the coolant gas and may therefore be deposited on the graphite surface, A second, significant pathway is via C-13(n,γ)C-14. Production from either O-16 or directly from O-17 via O-16(n,γ)O-17(n,α)C-14 is a minor, but non-trivial, route in coolants containing oxygen isotopes [i].

2.3 Chlorine

The use of either chlorine gas or freons in the purification process of graphite manufacture to remove certain metallic impurities as their volatile chlorides, can lead to residual Cl-35 contamination. Chorine-36, arising from activation of residual chlorine used in the graphite purification process, represents another significant contaminant of radioactive waste graphite. This isotope is important as it is long lived and poorly retarded by geological barriers [**Erreur ! Signet non défini.**].

It has been demonstrated experimentally for Vandellos sleeve graphite [ii] that a significant part of the Cl-36 content can be lost from small samples and powders, either through chemical reaction with atmospheric gases, diffusion or so-called ‘diffusion shock’ (in which is included the consequences of grinding up the sample).

- 0.013% Cl-36 lost in one year storage (silo) from a whole sleeve;
- 10% lost in ten days from material ground to 1mm;
- 80% lost in ten days from material ground to 100µm.

It should be noted that these results have not been corroborated with data from other sources [i]. In addition, it was stated that the position for Cl-36 requires further clarification; and it was suggested that the mobilisation of Cl-36 should be investigated further.

In addition to the activated radionuclides, graphite may also be contaminated with radionuclides arising within the reactor circuit, from either fuel element failure or activation products circulated in the coolant.

2.4 Metallic Radionuclides

Radioisotopes from corrosion products and lesser impurities [iii] may include: Ca-41, Fe-55, Ni-59, Ni-63, Co-60, Ag-110m, and Cd-109. Further, quantities of fission products (Sr-90, Zr-93, Tc-99, Pd-107, Cd-113m, Sn-121m, I-129, Ba-133, Cs-134, Cs-137, Pm-147, Sm-151, Eu-152, Eu-154, Eu-155, etc.), as well as some uranium and transuranic elements (mainly Pu-238, Pu-239, Pu-240, Pu-241, Am-241, Am-243, Cm-242, Cm-243 and Cm-244), will arise as a result of fuel failures during operation of the reactor, or from traces of uranium carried into the core on fuel-element surfaces after fabrication.

The radionuclide inventory of graphite can be divided into two categories:

Short lived isotopes.

These isotopes have short half-lives and decay to insignificant levels after a few tens of years. They may pose issues for handling graphite immediately after reactor shutdown, but are less relevant to the consideration of reactor graphite disposability due to NDA's current Safe Store policy which delays Magnox reactor decommissioning for 80 to 100 years. Short lived radionuclides typically include, Co-60 (half-life ~5.3 years) and H-3 (half-life ~12.3 years);

Long- lived isotopes.

These are key radionuclides for extraction during graphite treatment processing because they may pose radiological health issues through their release to the biosphere over the long term. These typically include, Cl-36 (half-life ~301,000 years), but principally C-14 (half-life ~5,730 years).

The source of radionuclides in graphite is likely to be a combination of the activation of an original impurity in the graphite (some of which may be gas trapped in the closed pores) together with contamination introduced in the coolant during reactor operation.

The radionuclide inventory of any sample of irradiated graphite should be understood prior to treatment to enable the most appropriate technology to be selected. The treatment of irradiated graphite may offer the opportunity to separate the important radionuclides (such as C-14) from the less problematic radionuclides.

2.5 Radiation Damages / Wigner Energy

Nuclear graphite components are polycrystalline in nature and their physical irradiation property changes are dominated by irradiation-induced changes to the graphite crystallites. The effect of irradiation on the crystallites is to expand in one direction and shrink, to a lesser extent, in the other direction. The consequence of this crystal dimensional change on the polycrystalline graphite component is critically dependent on the manufacturing route and the irradiation temperature. The changes in bulk volume lead to corresponding changes in density [iii].

The irradiation damage produced in graphite by energetic neutrons has been extensively studied [8] because of the use of graphite as a moderator in thermal nuclear reactors. The effects of irradiation on the structure of graphite have also been reviewed by Bradford and Steer [iv]. In the early stages of irradiation, crystal dimensional change rates may be slow and there will be little, if any, closure of porosity and increase in structural connectivity. As irradiation proceeds, the rate of graphite material growth in the c-axis will increase and the original thermal stress cracks produced during manufacture will be closed. The rate at which this occurs is initially slow but increases as irradiation proceeds. This crystal shape change in the graphite matrix drives closure of porosity and an increase in the structural connectivity, causing the modulus to increase slowly.

Under continued irradiation, expansion along the c-axis will begin to strain the graphite structural network. Where this strain cannot be relieved by the breaking and reforming of connecting bonds, new porosity will be generated by microcracking. It was highlighted that due to the distribution of the pore and crystallite sizes, pore generation will not occur simultaneously and uniformly in all regions of the material. Consequently some regions of the bulk material will still be undergoing pore closure whilst others undergo pore growth.

Bradford and Steer [iv] summarised that bulk dimensional change is the result of two processes; the underlying shrinkage of graphite crystalline and pore generation.

Irradiated graphite may contain stored Wigner energy. Wigner energy is energy stored within the graphite matrix in the form of displaced atoms. The quantity of accumulated stored energy is a function of fast neutron flux, irradiation time and temperature. The higher the irradiation temperature, the lower is the amount of stored Wigner energy. Wigner energy may be released if the graphite is heated to above its irradiation temperature, although a temperature in excess of 2000 °C is required to purge all Wigner energy [iii].

It has been stated that in Magnox-type reactors, graphite temperatures lie in the range 180 - 360ºC and accumulation of Wigner energy is limited to the cooler regions and even here the total stored energy saturates at levels which ensure that release rates upon heating are comfortably below the specific heat capacity [v].

The potential risk of triggering an inadvertent release of Wigner energy during graphite decommissioning and treatment is recognised as being small for the UK commercial reactor fleet. However, a management strategy for graphite may require the safe release of any stored Wigner energy to be taken into account.

3. Operational Conditions

3.1 CO2-Cooled Reactors

Draft document, text to be inserted by 2012

3.2 Helium-Cooled Reactors

Draft document, text to be inserted by 2012

3.3 Graphite irradiated under air and/or nitrogen (MTR, RBMK)

Draft document, text to be inserted by 2012

4. Methods for Analyses

4.1. Implantation of Simulants

Draft document, text to be inserted by 2012 ENS and INPL France

4.2. RAMAN

4.2.1. UoM Raman Spectroscopy Studies

Raman spectroscopy is a technique which relies on the inelastic (Raman) scattering of light by the molecules within a material and is therefore, a non-destructive technique. In carbon materials Raman is used to determine the degree of crystallinity ranging from poorly ordered carbon to high order in graphite and diamond. Principally, when a monochromatic beam of light impinges on a sample, a fraction of the light is scattered. The majority of this scattered light is elastically scattered. However, a small fraction is scattered at wavelengths different to that of the incident beam due to inelastic scattering. This change in frequency is called the Raman Effect. The resulting Raman spectrum corresponds to a particular bonding assignment. It is useful in the analysis of carbon- carbon bonding as one can ascertain information such as bonding type (sp^2/sp^3), structural characterisation, phase purity and crystallite size from the Raman spectrum.

The assignment of the band or peaks in the Raman spectrum is relatively straightforward in carbon materials and gives an insight into the molecular structure of carbon [10-11]. The G peak (located at 1580cm^{-1}) is dominant in single crystalline graphite and is due to the bond stretching of all sp^2 atoms both in the aromatic rings and chains. This peak typically exhibits a FWHM (Full Width at Half Maximum intensity) value less than 20cm^{-1} and is accompanied by the second harmonic (2D) at 2700cm^{-1} which is indicative of highly crystalline graphite. In polygranular graphite and baked carbon material there is a D-peak present around 1350cm^{-1}. This is assigned to the breathing node of disordered sp^2 atoms in rings and may increase in intensity relative to the G-peak with decreasing crystallite size [11].

The degree of disorder within graphite has been studied by Tunstra and Koening [12] who noted the ratio of the D-peak intensity to that of the G-peak varied inversely with crystallite size (L_a), where crystallite size was obtained from the FWHM of x-ray diffraction peaks:

$$\frac{I(D)}{I(G)} = \frac{C(\lambda)}{L_a} \qquad \textbf{(1)}$$

Where C is the bond force constant of 4.4 nm at λ=514.5nm

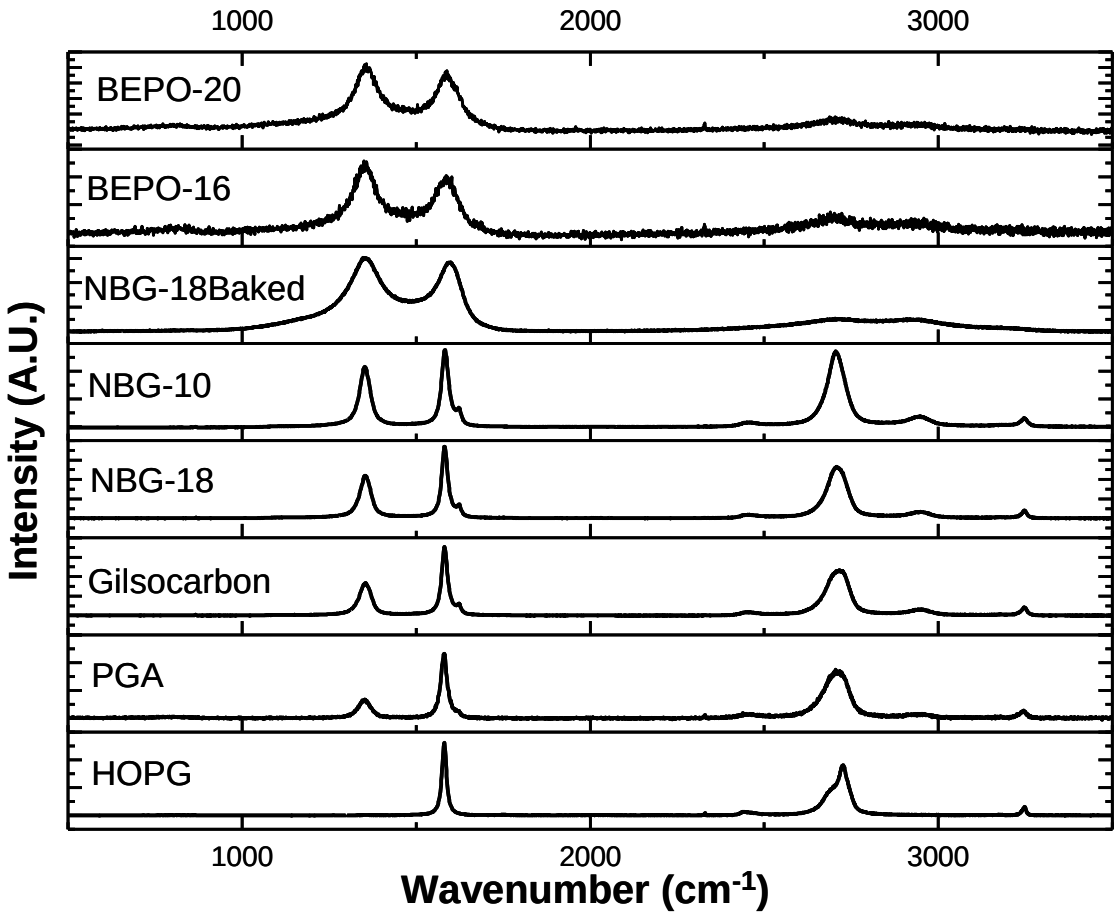

FIGURE 1 - Raman Spectra of various nuclear graphite grades including VHTR grades and UK irradiated BEPO graphite.

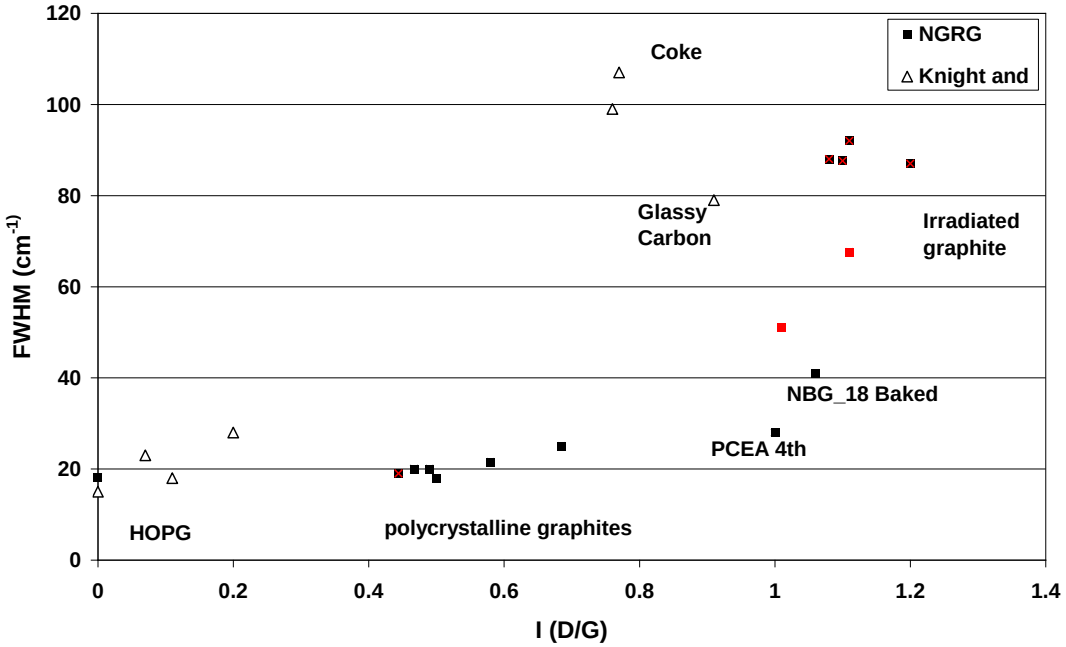

FIGURE 2 - Raman ratio of I(D)/(G) against Full width half maximum of the G-peak to show the structural disordered of various nuclear graphite grades including VHTR grades and UK irradiated BEPO graphite.

Figure 1 shows the Raman spectra of several polygranular nuclear graphites and irradiated nuclear graphite from the British Experimental Pile grade Zero (BEPO) reactor. A reduction in the G-peak intensity relative to virgin graphite and low irradiation BEPO graphite is evident with increasing fluence. The FWHM of the G-peak also increases in graphite samples which have undergone fast neutron irradiation. The irradiated graphite samples also show the magnitude of the D-peak increases with increasing fluence. This is indicative of increased structural disorder from the presence of both sp^2 and amorphous sp^3 carbon phases. Figure 4shows the Raman G-peak FWHM as a function of the I (D)/ (G) ratio for various graphite and coke materials. Results from this group are compared with those of Knight and White [13]. The highly ordered pyrolytic graphite (HOPG) shows little peak broadening and is directly comparable with that of Knight and White. The general behaviour of unirradiated polycrystalline nuclear graphite is that the FWHM is less than $20cm^{-1}$ and the I (D) / (G) ratio is below one. Neutron irradiated samples show larger values both in terms of FWHM and I(D)/I(G) ratio, similar baked graphite, coke and glassy carbon. These methods are now being

used to quantify the effects of fast neutron irradiation and graphite manufacture on crystallite size and order/disorder within graphite crystals.

4.2.2. ENS RAMAN Studies

Principally, ENS's work started by characterizing the virgin nuclear graphite of Saint Laurent des Eaux, France (SLA2) using Raman microspectrometry. This technique was particularly attractive due to the high spatial resolution (~ 1 µm) achieved and that Raman provides less averaged information, in comparison with X-ray diffraction (XRD). Moreover, analyses were quick, operationally straightforward, non-destructive and requiring minimal sample preparation.

Compared to a single crystal of graphite (as for the Highly Oriented Pyrolytic Graphite (HOPG)), Raman spectrum of nuclear graphite exhibited additional bands labelled D for "Defect" bands, which are known to be characteristic for finite crystals of graphite. The polarization of the laser spot was used to distinguish preferentially oriented from randomly oriented crystals. Our result ensured that the nuclear graphite is composed of small crystallites more or less randomly oriented in the area of the laser spot. This aspect has been confirmed by X-ray Diffraction analyses.

Raman mapping of virgin nuclear graphite was performed, using the structural parameter R_2, (D_1 area relative to the whole bands area). Compared to HOPG, virgin nuclear graphite featured a clear repartition on the defect band area. This showed the heterogeneity of the nuclear graphite, at a micrometric scale, in terms of the organization degree. This variation could be directly related to the composition of the nuclear graphite consisting in two main phases: the binder (coal-tar pitch) and the filler (petroleum coke) heated at 2800°C. Petroleum cokes are generally the more graphitizable of the two, and this aspect could give a noticeable decrease of the defect bands in Raman spectrum. Additional experiments are now initiated by combined Raman mapping, scanning electron microscopy and optical microscopy in order to distinguish between the binder and the filler in the nuclear graphite.

In order to select any treatment option for irradiated nuclear graphite, it is necessary to obtain a comprehensive understanding of the character in terms of the nanostructure of raw and modified graphite. Ion irradiation beam (implantation) may provide an effective way of the structural modification of graphite, where the structural defect could be similar to those induced by neutrons irradiations at varying fluences and temperatures. Moreover, such implantation can introduce a wide range of defects in a controlled manner.

Raman analyses showed an increase of defect bands with fluence in room temperature conditions, resulting in a disorder increase in the graphitic structure, until a complete amorphization for higher fluences characterized by an asymmetric broad single band. Compared to X-ray diffraction, Raman microspectrometry appears as particularly sensitive to both the disorder and the amorphization, and may be achieved on very small volumes of matter (less than 0.1 μm^3).

A more interesting finding occurred when we implanted the nuclear graphite at various temperatures. At high implantation temperatures (up to 600°C), the defect band in Raman spectrum decreased significantly suggesting that graphite defects recombine as fast as they form.

Analysis from Transmission electron microscopy (TEM) showed particularly interesting findings, in particular the 002 lattice fringe (LF) mode that allowed a direct imaging of the polyaromatic layers profile and consequently the access to the multiscale organization in the nanometer-micrometer range. The observation of the nanostructural changes caused by the ion beam irradiation at the surface or near the surface (implantation depth about 1 µm) however, was not easily achievable by the conventional techniques such as hand grinding, ultramicrotomy and mechanical abrasion or ion thinning. The process which provided a great advance in the study of the ion-implanted graphite was the use of thin sections prepared by the focused ion beam (FIB) technique. In fact, its very important benefit was the easy and direct control of the choice of the area, the sample orientation according to the beam and the specimen thickness during ion milling (less than 100 nm that making it electrons transparent). By using thin sections prepared by FIB technique, we were be able to image directly, for the

first time, the structural modification due to implantation at the nanometre scale; this can be considered as a great improvement in the characterization of the ion-implanted graphite.

Our results showed a dramatic change of the polyaromatic layers organization at the surface, where the density of ^{37}Cl implantation was maximal. The graphite structure was strongly damaged without being completely amorphous: only short nanometer sized fringes forming small BSU (stacks of 2-3 layers) were visible and these stacks were strongly disoriented, losing the lamellar nanostructure of the virgin graphite. Geometrically speaking, such cross-linked BSUs form nanopores that could be considered as potential sites for radionuclides trapping.

The decrease of L_a, the coherent domain (BSU) diameter was also confirmed after ion beam irradiation by the measurement of the rotation moirés fringes in the 11DF dark field images, which was in perfect correlation with Raman results.

As we expected, the nanometer scale examination appeared extremely important to explore as it was planed at the beginning within the framework of Carbowaste program, based on our knowledge in carbon materials.

Irradiated graphite studies have recently begun on G2 samples issued from the nuclear reactor of Marcoule, France. The nuclear graphite was irradiated at a temperature close to 300°C. Compared to virgin graphite characterized by a weak defect band, Raman spectrum of irradiated graphite shows a slight increase of this later. This aspect has been confirmed by TEM observations with the 002 LF mode, for which the polyaromatic layers were slightly distorted. We attributed this relatively weak structural degradation of this irradiated graphite (about 4dpa) to the irradiation temperature.

presently, our experiments are in progress to study other irradiated graphite depending on their location in the UNGG reactor (which were submitted to other irradiation degrees and/or temperatures), and from other types of reactors. For this, a HRTEM image analysis will be used to acquire more quantitative structural data.

4.3. XPS

To be inserted: Comments required from all Wp3

4.4. Porosimetry

Manufactured nuclear graphite has a finite porosity prior to irradiation. Extensive networks of interconnected pores, leading from the surface to the core are also a common feature. These are referred to as 'open' pores, isolated pores being referred to as 'closed'. The graphite structure in terms of open and closed porosity for the main UK graphite is provided in [vi]:

In Magnox reactors, two types of graphite were used in core construction:

- Pile Grade A (PGA), primary graphite used for moderators
- Pile Grade B (PGB), mainly used for reflectors

Both materials were manufactured by a similar process, but PGA has a higher density than PGB [**Erreur ! Signet non défini.**]. During manufacture PGA material was subject to additional heat treatment to reduce porosity and therefore increase its density. The resulting virgin PGA material has a porosity of approximately 20% (vii).

A significant proportion of the porosity is open to the coolant circuit in gas-cooled reactors. In consequence, deposition of activated materials can occur both upon the geometrical surfaces of graphite components and on internal pore surfaces, especially where there are permeable gas flows through the graphite blocks due to pressure differentials [i].

Most of the graphite surface area of nuclear graphite is contained within the graphite pores. Therefore, the majority of radiolytic oxidation is likely to take place at the surface of the open pores of the graphite core. During radiolytic oxidation, the graphite that forms the surface of the open pore is eroded by interaction with coolant CO_2 Radiolysis of CO_2 produces an oxidising species (O_x) which can either react with an adjacent graphite surface, or be deactivated by a sequence of reactions involving CO. Attack is most aggressive in small pores where the surface area: volume ratio is high. Grain boundaries are also aggressively eroded, enabling open pore networks to grow by linking together with closed pores. The corrosion rate of graphite can reasonably be expected to be a function of the accessible pore volume.

It has been well documented that radiolytic oxidation leads to graphite weight loss. In Magnox graphite the weight loss originates from the opening up by oxidation of the open-pore structure

and, at the higher weight losses, much, if not all, of the closed porosity is also opened up. The dependence of oxidation rate of open pore volume has been demonstrated for PGA graphite in CO_2. It has been shown that up to 40 % of the initially closed-pore volume can become accessible by 2 % weight loss in CO_2 [viii].

The study of the pore morphology in nuclear graphite has traditionally been carried out using methods such as:

- Optical microscopy;
- Scanning electron microscope (SEM); and
- Transmission electron microscope (TEM).

Although valuable, these techniques only reveal details of the surface of the structure, and do not give a 3-D image. Such a 3-D image may be provided by X-ray micro-Tomography (XRμT), which may be applied to study the microstructure of nuclear graphite. This technique has been used by Sun *et al.* [ix] to provide a non-destructive measure of the porosity of graphite before and after irradiation.

5. Locations and Chemical Bounds before Treatment

/interpretation of analyses to be inserted by all partners/

5.1 Tritium

5.2 Radiocarbon

5.3 Chlorine

5.4 Metallic Radionuclides

Inspection of a typical reconstructed CT volume of graphite (Figure 3) shows clearly identifiable pores within the graphite matrix. These can be segmented and examined quantitatively in three dimensions (Figure 4). In some samples areas of high attenuation were

observed (Figure 5). These high attenuation areas could be broadly divided into 2 types; spots and smears. Spots were highly localised areas with a greyscale value (attenuation) that saturated at the maximum, and smears were larger areas where the greyscale value was noticeably higher than the average of the surrounding material (Figure 6). Attenuation is proportional to the density of the material of constant atomic number, and the attenuation in these areas is too high for them to be due variations in graphite density. It was important to determine the composition of the high attenuation areas to determine their origin. In the reactor certain elements can be transmuted into radioactive isotopes, and their location and ease of transport within the porous microstructure have implications for graphite decommissioning

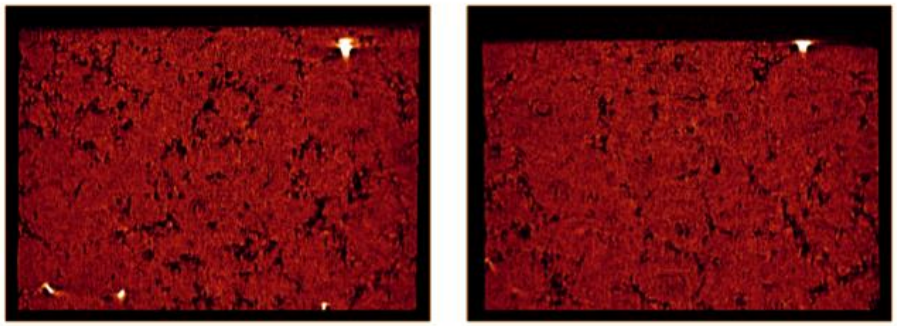

FIGURE: 3 - Location of a high attenuation spot; a) before grinding; b) after grinding.

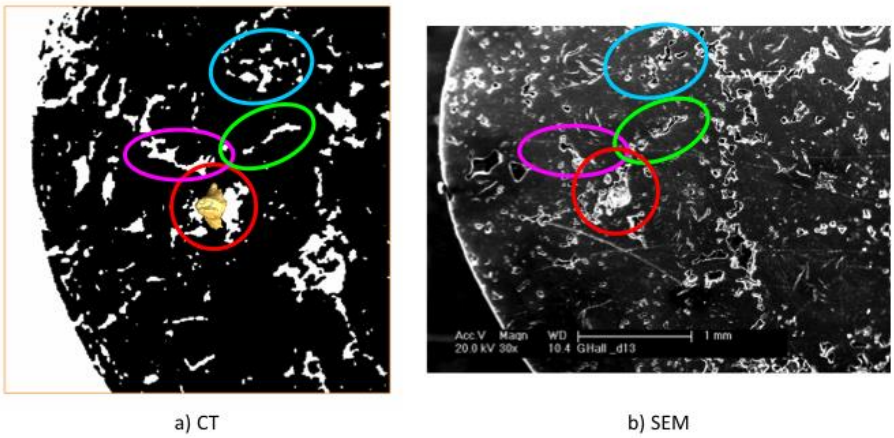

FIGURE: 4 - Matching of pores (purple, green, and blue ellipses) to locate the high attenuation spot (red circle); a) 2D CT slice; b) SEM.

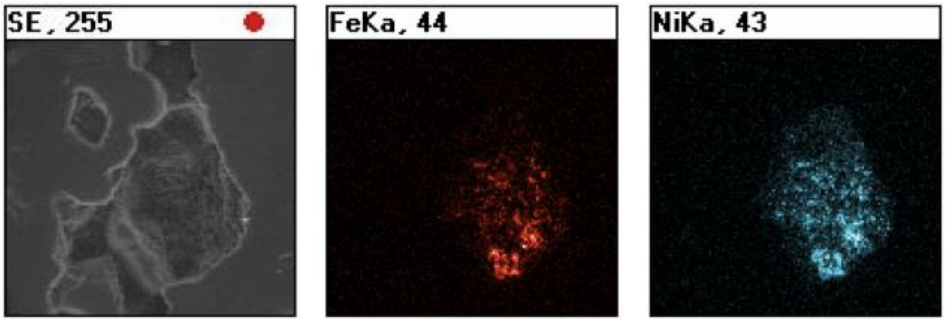

FIGURE: 5- EDXS analysis of a high attenuation spot showing concentrations of iron (Fe) and nickel (Ni).

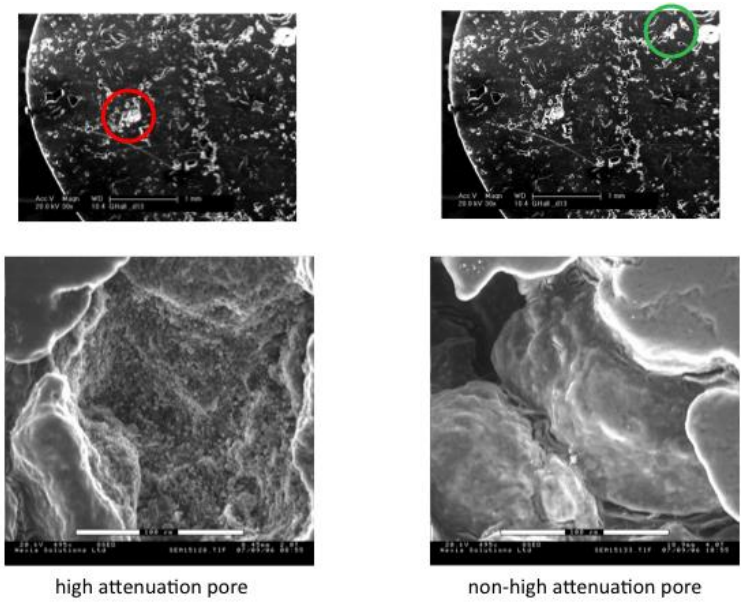

FIGURE: 6 - SEM images of the high attenuation spot and of a "normal" pore, showing a crystalline shell structure within the high attenuation spot.

A CT scanned sample with a high attenuation spot close to the surface was selected (Figure 3a). The sample was the mechanically ground until the spot was exposed (Figure 3b). By examining a 2D slice through the CT reconstruction of the sample, the pores surrounding the high attenuation spot were used to locate the high attenuation spot when the sample was placed in an SEM (Figure 14) for elemental analysis. The composition of the high attenuation spot was then examined using energy dispersive X-ray spectroscopy (EDXS) *in situ* in the SEM. The EDXS spectrum showed that the high attenuation spot was rich in iron and nickel (Figure

5); these elements were found only in the high attenuation areas. Further examination of the SEM micrographs showed that the high attenuation spot was not solid, but was a hollow pore with crystalline facets coating the inner surface (Figure 6). This is likely to have been deposited during graphitisation when metallic impurities vaporised.

6. Locations and Chemical Bounds after Treatment

/interpretation of analyses/

6.1 Tritium

6.2 Radiocarbon

6.3 Chlorine

6.4 Metallic Radionuclides

7. Evaluation of Treatment Options

8. Summary

/FZJ/ Publishable summary

9. References

i Bradbury, D., and Wickham, A.J. *Graphite Decommissioning: Options for Graphite Treatment, Recycling, or Disposal, including a discussion on Safety-Related Issues*. EPRI, Palo Alto, CA: 2006. 1013091.

ii Rahmani L, "Chlorine Degassing from Nuclear Grade Graphite"; presented at 6th International Nuclear Graphite Specialists' Meeting, Chamonix, France, September 2005,

iii IAEA TECDOC-1521. *Characterization, Treatment and Conditioning of Radioactive Graphite from Decommissioning of Nuclear Reactors*. September 2006.

iv Bradford, M.R., and Steer, A.G. A structurally-based model of irradiated graphite properties. Journal of Nuclear Materials 381 (2008) 137–144.

v Wickham A.J., "Caring for the Graphite Cores"; Proc. Seminar 'The Review of Safety at Magnox Nuclear Installations', London, March 1989, I.Mech E. pp. 79-8715

vi Marsden, B.J., Hopkinson, K, L., Wickham, A.J. (March 2002) The Chemical Form of Carbon-14 within Graphite. Serco Assurance. SA/RJCB/RD03612001/R01 Issue 4.

vii Marsden, B.J., Production, Location and Retention of Carbon 14 in irradiated Graphite, A report for UKAEA, SERCO Assurance, SA/RJCB/RD03510001/R01 Issue 2, July 2002.

viii Standring, J., Ashton, B.W., The Effect of Radiolytic Oxidation by Carbon Dioxide on the Porosity of Graphite, Carbon, 3, 157-165, 1965.

ix Sun,L., Hodgkins, A., Marrow, J., Fok, A.S.L., and Marsden, B.J. AN EXPERIMENTAL STUDY ON THE POROSITY NETWORKS IN NUCLEAR GRAPHITE in 2nd International Topical Meeting on HIGH TEMPERATURE REACTOR TECHNOLOGY. Beijing, CHINA, September 22-24, 2004.

1. APPENDICES